Supplementary Information

Heterometallic thiacalix[4]arene-supported $Na_2Ni^{II}_{12}Ln^{III}_2$ clusters with vertex-fused tricubane cores (Ln = Dy and Tb) †

Kecai Xiong,[a,c] **Xinyi Wang**,[b] **Feilong Jiang**,[a] **Yanli Gai**,[a,c] **Wentao Xu**,[a] **Kongzhao Su**,[a,c]

Xingjun Li,[a,c] **Daqiang Yuan**[a] **and Maochun Hong**[*a]

[a] State Key Laboratory of Structure Chemistry, Fujian Institute of Research on the Structure of Matter, Chinese Academy of Sciences, Fuzhou, 350002, China.

[b] State Key Laboratory of Coordination Chemistry, School of Chemistry and Chemical Engineering, Nanjing University, Nanjing, 210093, China.

[c] Graduate School of the Chinese Academy of Sciences, Beijing, 100049, China.

- Corresponding author:

  E-mail: hmc@ fjirsm.ac.cn.

  Tel: +86-591-83714605; Fax: +86-591 / 8379 4946

Experimental section

Materials and Measurements

p-tert-Butylthiacalix[4]arene was prepared according to literature methods,[S1] while other chemicals were of reagent-grade quality obtained from commercial sources and used without further purification. Elemental analyses were performed with a German Elementary Varil EL III instrument. IR spectrum were recorded in the range 4000–400 cm^{-1} with a Magna 750 FT-IR spectrometer using KBr pellets. The powder X-ray diffraction (PXRD) were recorded by a RIGAKU-DMAX2500 X-ray diffractometer using Cu Kα radiation (λ = 0.154 nm) at a scanning rate of 3°/min for 2θ ranging from 2° to 50°. Magnetic susceptibilities were measured on polycrystalline samples with the Quantum Design PPMS-9T and MPMS-XL systems. All experimental magnetic data were corrected for the diamagnetism of the sample holders and of the constituent atoms according to the Pascal's constants.

Syntheses of complexes 1-2

Complex 1: A mixture of H_4BTC4A (0.1 mmol, 72 mg), $NiCl_2$•$6H_2O$ (0.4 mmol, 95 mg) $Dy(OAc)_3$•$6H_2O$ (0.3 mmol, 132 mg) and Na_2CO_3 (0.2 mmol, 21 mg) in DMA/CH_3CN/Et_3N (6/3/0.5 mL) was sealed in a 25 mL Teflon-lined bomb at 130 □ for 6 days, then cooled slowly at 4 ℃h^{-1} to room temperature. Slow concentration of the filtrate at room temperature for several days and then green blocky crystals of complex **1** (55 mg) were obtained in 33% yield based on H_4BTC4A. Anal. Calcd. for complex **1**: calcd. C, 44.32; H, 5.45; N, 4.31. found C, 44.48; H, 5.19; N, 4.14. IR (KBr disk, ν cm^{-1}): 3439 (m), 3256 (m), 2960 (S), 2901 (m), 2872 (m), 1649 (S), 1586 (S), 1460 (s), 1361 (m), 1319 (m), 1305 (m), 1258 (s), 1188 (m), 1130 (w), 1089 (w), 1016 (m), 911 (w), 883 (w), 865 (w), 834 (m), 750 (m), 733 (w), 672 (w), 590 (w), 542 (w).

Complex 2: Equivalent synthesis procedures were carried out employing $Tb(OAc)_3$•$6H_2O$ (0.3 mmol, 131 mg) to obtain the corresponding products. Colorless block crystals of complex **2** (47 mg) were obtained in 28% yield based on H_4BTC4A. Anal. Calcd. for complex **2**: calcd. C, 44.38; H, 5.46; N, 4.31. found C, 44.26; H, 5.30; N, 4.26. IR (KBr disk, ν cm^{-1}): 3439 (m), 3256 (m), 2960 (S), 2901 (m),

2872 (m), 1649 (S), 1586 (S), 1460 (s), 1361 (m), 1319 (m), 1305 (m), 1258 (s), 1188 (m), 1130 (w), 1089 (w), 1016 (m), 911 (w), 883 (w), 865 (w), 834 (m), 750 (m), 733 (w), 672 (w), 590 (w), 542 (w).

X-ray Data Collection and Structure Determination

Data collection for complexes **1** and **2** were performed on Rigaku-CCD diffractometers equipped with graphite monochromated Mo-Kα radiation (λ = 0.71073 Å) by using the ω-scan mode at 123 K. All absorption corrections were applied using the *CrystalClear* program. The structures were solved by direct methods, the metal atoms were located from the E-maps, and other non-hydrogen atoms were derived from the successive difference Fourier peaks. The structures were refined on F^2 by full-matrix least-squares using the *SHELXTL*-97 program package.[S2] All non-hydrogen atoms were refined anisotropically except some solvent molecules and some disordered atoms, and hydrogen atoms of the organic ligands were generated theoretically onto the specific atoms and refined isotropically with fixed thermal factors. Some hydrogen atoms on solvent molecules cannot be generated and were included in the molecular formula directly. It was not possible to model all the disordered solvent molecules appropriately. The diffraction data were treated by the ‘‘SQUEEZE’’ method as implemented in PLATON to remove diffuse electron density associated with these badly disordered solvent molecules.[S3] This has the effect of dramatically improving the agreement indices. Solvent molecules in complexes **1** and **2** were estimated from the result of PLATON–SQUEEZE and the data of elemental analyses, and were included in the molecular formula directly. A number of restraints were applied owing to disorder in the solvent molecules. In addition, the high R_1 and wR_2 factors of complexes **1** and **2** might be due to the weak high-angle diffractions and the disorder of some solvent molecules.

Solvent assignment for complexes 1 and 2:

SQUEEZE RESULTS (APPEND TO CIF) of **1**

loop_

_platon_squeeze_void_nr

_platon_squeeze_void_average_x

_platon_squeeze_void_average_y

_platon_squeeze_void_average_z

_platon_squeeze_void_volume

_platon_squeeze_void_count_electrons

1	0.386	0.188	0.639	530.9	28.5
2	0.386	0.311	0.139	530.9	26.0
3	0.614	0.688	0.861	530.9	32.3
4	0.614	0.811	0.361	530.8	30.4
5	0.827	0.099	0.301	23.2	0.7
6	0.828	0.401	0.801	23.2	0.4
7	0.602	0.122	0.500	7.0	0.0
8	0.758	0.168	0.334	6.8	0.5
9	0.759	0.333	0.833	6.9	0.5
10	0.602	0.378	0.000	6.9	-0.2

_platon_squeeze_details

;

SQUEEZE RESULTS (APPEND TO CIF) of **2**.

loop_

_platon_squeeze_void_nr

_platon_squeeze_void_average_x

_platon_squeeze_void_average_y

_platon_squeeze_void_average_z

_platon_squeeze_void_volume

_platon_squeeze_void_count_electrons

1	0.766	0.147	0.691	313.5	17.7
2	0.234	0.853	0.309	313.6	17.4
3	0.766	0.353	0.191	313.6	16.7
4	0.234	0.647	0.809	313.5	17.5
5	0.019	0.202	0.945	191.8	21.7
6	0.019	0.298	0.444	191.9	22.0

7	0.981	0.702	0.556	192.0	21.8
8	0.981	0.798	1.055	191.9	22.3
9	0.304	0.116	0.309	35.7	2.7
10	0.104	0.123	0.499	12.3	0.6

_platon_squeeze_details

;

Complexes **1** and **2** are isomorphous. PLATON/SQUEEZE estimated the solvent-accessible region void to contain (28.5+26.0+32.3+30.4) and (17.7+17.4+16.7+17.5+21.7+22.0+21.8+22.3) electrons for complexes **1** and **2**, respectively. The electron densities were tentatively modeled as two dma and four CH_3CN molecules (z = 4; half dma and one CH_3CN molecules per asymmetric unit) which account for (26+26+22+22+22+22) electrons. The final chemical formula of **1** and **2** were calculated from the SQUEEZE results combined with the elemental analyses data.[S4]

S1 P. Lhotak, T. Smejkal, I. Stibor, J. Havlicek, M. Tkadlecova and H. Petrickova, *Tetrahedron Lett.*, 2003, **44**, 8093-8097.

S2 G. M. Sheldrick, SHELXS 97, *Program for crystal Structure Solution* and *Program for crystal Structure Refiniement*, 1997, University of Göttingen.

S3 P. van der Sluis and A. L. Spek, *Acta Cryst. Sect. A.* 1990, **46**, 194-201.

S4 (a) Y. F. Bi, X. T. Wang, W. P. Liao, X. F. Wang, X. W. Wang, H. J. Zhang and S. Gao, *J. Am. Chem. Soc.* 2009, **131**, 11650; (b)Y. F. Bi, S. C. Du and W. P. Liao, *Chem. Commun.*, 2011, **47**, 4724.

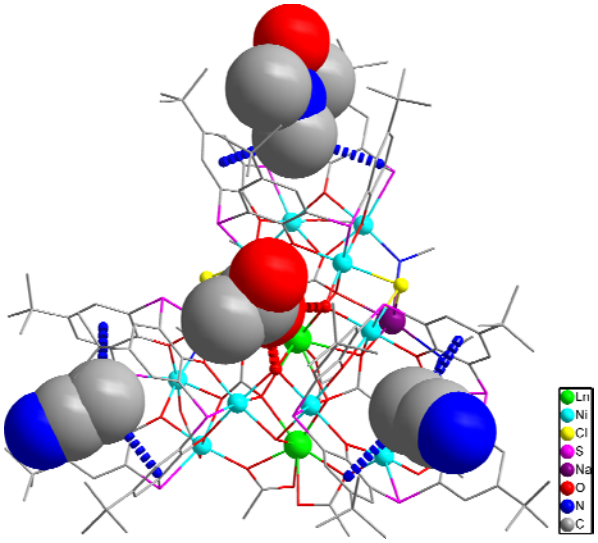

Fig. S1 Two MeCN and one DMA molecules penetrate slantwise into three thiacalix[4]arene cavities stabilized by C-H···π interactions (blue dashed), while one acetate counter anion locates above the tricubane core *via* hydrogen bonds (red dashed).

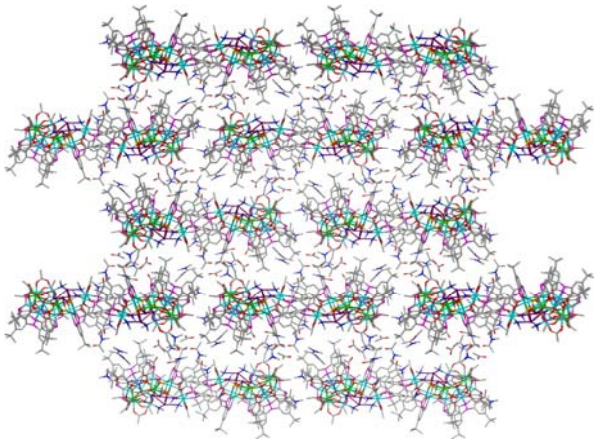

Fig. S2 Extended structure of complex **1** showing self-assembly through an up-down fashion into a bilayer array with ABAB··· mode view along *a* axis. Hydrogen atoms are omitted for clarity.

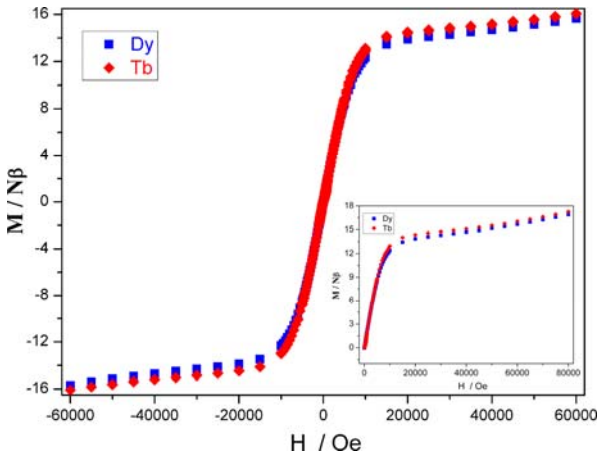

Fig. S3 Field dependence of the magnetization of complex **1** (Dy) and **2** (Tb) measured at 2 K in the -60 – 60 kOe range. Inset: the *M-H* plots of complex **1** and **2** at 2 K.

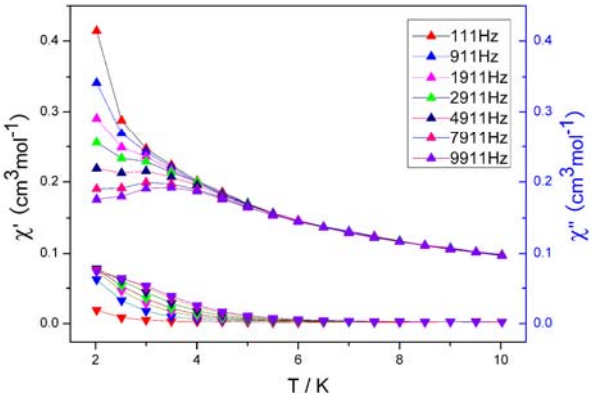

Fig. S4 Temperature dependence of the in-phase (top) and out-of phase (bottom) components of the ac magnetic susceptibility for complex **1** in a zero applied dc field and an ac field of 3 Oe.

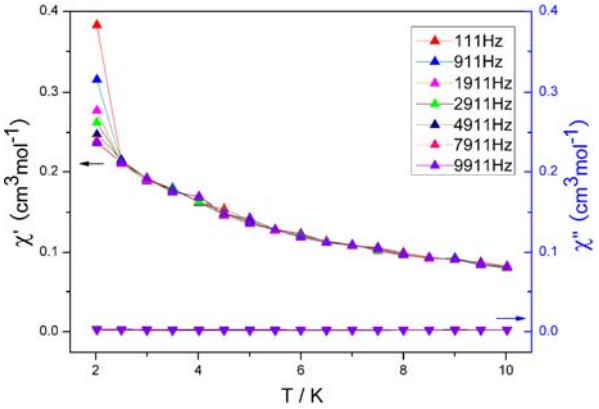

Fig. S5 Temperature dependence of the in-phase (top) and out-of phase (bottom) components of the ac magnetic susceptibility for complex **2** in a zero applied dc field and an ac field of 3 Oe.

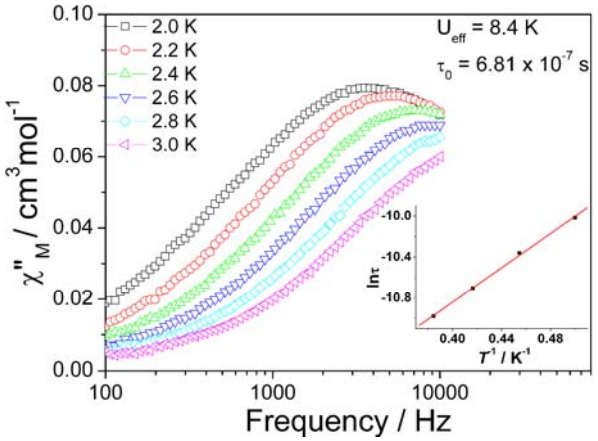

Fig. S6 Frequency dependence of the out-of-phase ac susceptibility of complex **1** under zero-dc field. Inset: Relaxation time, ln(τ), versus T^{-1} plot for complex **1** under zero-dc field. The solid line is fitted with the Arrhenius law (see text).

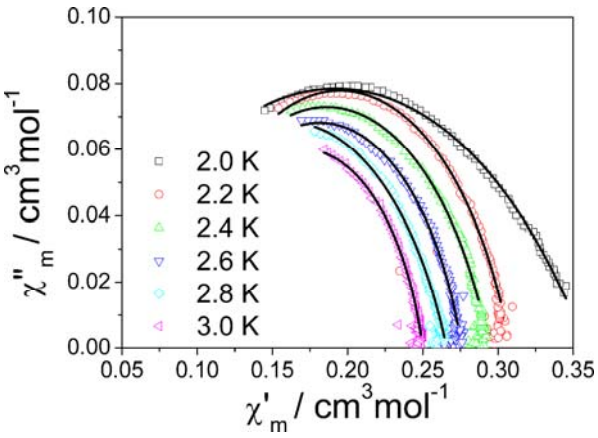

Fig. S7 Cole–Cole plots for complex **1** measured below 3 K and zero-dc field; the solid lines are the best fits to the experimental data, obtained with the generalized Debye model.

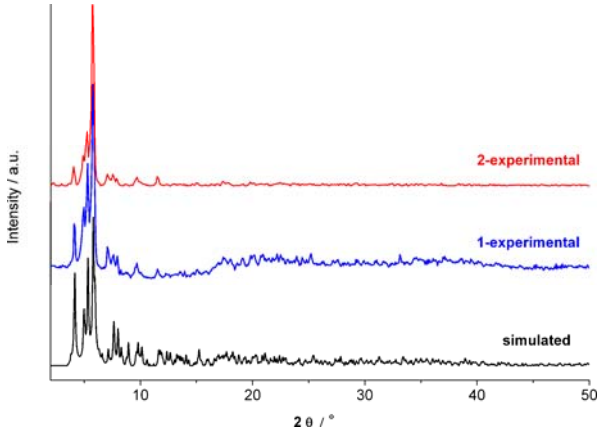

Fig. S8 PXRD of complexes **1** and **2**.